Hard X-ray microprobe highlights the structure of multi-quantum wells in electroabsorption-modulated lasers for optoelectronics

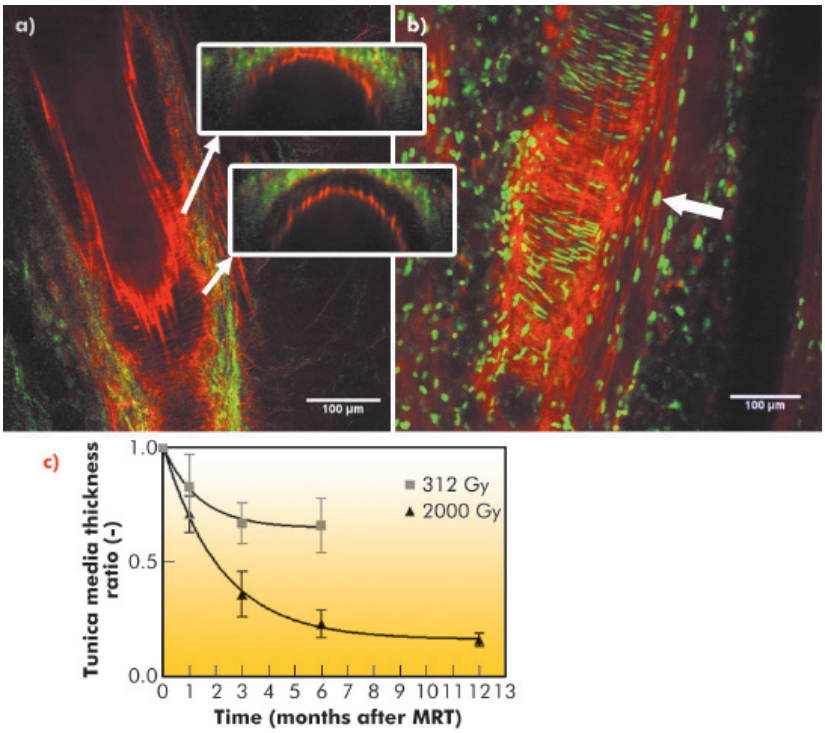

Fig. 129: Longitudinal sections taken three months after microplanar irradiation (2000 Gy). a) Elastic fibres (red) and collagen fibres type I and III (SHG, green) 26 µm below the external surface of the artery. Inserts: Cross sections at the level of the beam path and the valley; the (dark) TM in the beam path is thinner than in the valley region. b) Image 16 µm below the external surface of the artery. Elastic fibres (red) are diffusely stained in the beam path. The density of the green, elongated-shaped VSMC nuclei is higher in the valleys than in the darker beam path. c) Mean tunica media thickness ratio (microbeam path/valley, ± one standard deviation) versus time after irradiation, 312 Gy (■) and 2000 Gy (▲) dose groups.

References

[1] D.N. Slatkin, P. Spanne, F.A. Dilmanian and M. Sandborg, *Med Phys* **19**, 1395-1400 (1992).

[2] R. Serduc, P. Verant, J.C. Vial, R. Farion, L. Rocas, C. Remy, T. Fadlallah, E. Brauer, A. Bravin, J. Laissue, H. Blattmann and B. van der Sanden, *Int J Radiat Oncol Biol Phys* **64**, 1519-1527 (2006).

[3] W. Denk, J.H. Strickler and W.W. Webb, *Science* **248**, 73-76 (1990).

[4] C. Ricard, J.C. Vial, J. Douady and B. van der Sanden, *J Biomed Opt* **12**, 064017 (2007).

We have evaluated the effect of MRT on the artery wall of living mice using intravital microscopic techniques: two-photon microscopy (2PM) and second harmonic generation imaging (SHGI) [3]. A new two-photon imaging protocol was used for a more sensitive and deeper detection of elastic fibres in the artery wall using sulforhodamin-B [4]. In parallel, VSMC in the artery wall were detected after nuclei staining with Hoechst 33342.

The left hind leg of healthy mice including the saphenous artery was irradiated by an array of 26 microbeams of synchrotron X-rays (50 µm-wide, spaced 400 µm on centre) with peak entrance doses of 312 Gy and 2000 Gy. During 12 months after irradiation, the artery remained patent, but narrow VSMC segments in the tunica media that were in the microplanar beams paths became atrophic and fibrotic in a dose-dependent pattern (**Figure 129**). The wide tunica media segments between the microbeam paths hypertrophied.

Mice hind leg arteries tolerate microbeam peak doses of up to 2000 Gy delivered by spatially fractioned micro planar beams in a single session without developing occlusions within 1 year, in contrast to the deleterious consequences of comparable doses delivered by broad-beam X-rays. The permanent sequelae of microplanar irradiation appear to be confined to microscopic segments of the tunica media (layer with VSMC) and tunica adventia (outermost collagen layer of the artery that showed fibrosis). Clinical risks of long-delayed disruption or occlusion of non-targeted arteries from microbeam radiation therapy will prove less than corresponding risks from broad-beam radiosurgery, especially if peak doses are kept below 3 hectogray.

Materials science

Structure of multi-quantum wells in electroabsorption-modulated lasers for optoelectronics

Multi-quantum well (MQW) structures based on quaternary III-V semiconductor alloys are widely used in optical communication systems. Optoelectronic devices often require the integration of two different functions in the same chip. The selective area growth (SAG) technique gives excellent results for such monolithic integration [1]. SAG exploits

the perturbation of the growth fluxes induced by a dielectric mask. When the metallorganic precursors collide with the dielectric mask, they are deflected and migrate through the unmasked semiconductor where the growth starts. In this way, the reactive species coming from the gas phase are enriched by those deflected by the mask and the result is a variation in composition and thickness of semiconductors grown near (SAG region) and far (field region) from the mask.

The electroabsorption modulated laser (EML), obtained by monolithic integration of an electroabsorption modulator (EAM) with a distributed feedback laser (DFB), is one of the most promising applications of SAG. A voltage modulation applied to the EAM switches it between an opaque and a transparent state by means of the Stark effect and ensures the modulation of the DFB laser emission, allowing long-distance communication (up to 80 km) at high frequency (10 Gb/s). The SAG EML device investigated here is an $Al_{xw}Ga_{yw}In_{1-xw-yw}As/Al_{xb}Ga_{yb}In_{1-xb-yb}As$ (compressive-strained well/tensile-strained barrier) MQW structure grown on InP by metallorganic vapour phase epitaxy. The mask used for the growth (Figure 130a) featured 20 μm wide SiO_2 stripes with a 30 μm opening width between them.

X-ray fluorescence (XRF) maps (Figure 130b) reveal that Ga K_α and As K_β counts are higher in the SAG region owing to material enrichment caused by the SiO_2 stripes. The effectiveness of the SAG technique in modulating the chemical composition of the quaternary alloy is proven by the map reporting the ratio between Ga and As counts in which a gradient in the average well/barrier chemical composition is clearly visible. Since the Ga/As ratio is lower in the SAG region than in the field, we can assert that the average Ga content of the MQW structure progressively increases by moving from the SAG to the field (along the Y-line showed in Figure 130a).

Principal publication and authors
L. Mino (a), D. Gianolio (a), G. Agostini (a), A. Piovano (a), M. Truccato (b), A. Agostino (c), S. Cagliero (c), G. Martinez Criado (d), S. Codato (e) and C. Lamberti (a), *Adv. Mater.* **22**, 2050-2054 (2010).
(a) Department of Inorganic, Materials and Physical Chemistry, University of Turin (Italy)
(b) Department of Experimental Physics, University of Turin (Italy)
(c) Department of General and Organic Chemistry, University of Turin (Italy)
(d) ESRF
(e) Avago Technologies Italy S.r.l., Turin (Italy)

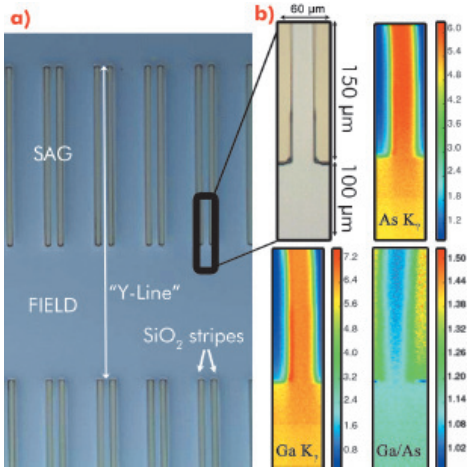

Fig. 130: a) Optical micrograph of the SiO_2 stripes-patterned InP substrate allowing SAG growth. The black rectangle, magnified in part (b), shows the region sampled in the XRF maps. b) Spatial maps of the fluorescence counts of the principal element's lines.

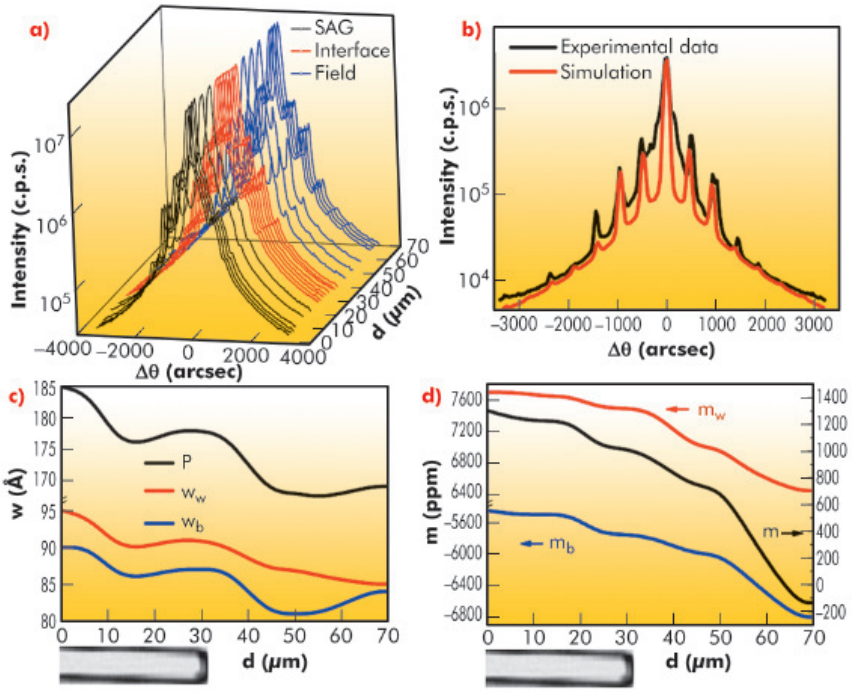

Fig. 131: a) XRD patterns collected along the Y-line starting 30 μm before the end of the stripes in the SAG region. b) Experimental and simulated XRD patterns in the field region. c) Barrier and well widths and period as a function of the position along the Y-line, obtained by simulation of the 35 experimental XRD patterns. d) As part c) for the well, barrier and overall mismatches.

References
[1] M.E. Coltrin and C.C. Mitchell, *J. Crystal Growth* **254**, 35–45 (2003).
[2] C. Ferrari and C. Bocchi, in: *Characterization of Semiconductor Heterostructures and Nanostructures*; C. Lamberti, Ed.; Elsevier: Amsterdam, 93–132 (2008).
[3] L. Mino, A. Agostino, S. Codato and C. Lamberti, *J. Anal. At. Spectrom.* **25**, 831-836 (2010).
[4] L. Mino, D. Gianolio, G. Agostini, A. Piovano, M. Truccato, A. Agostino, S. Cagliero, G. Martinez-Criado, F. d'Acapito, S. Codato and C. Lamberti, Small 7, in press, DOI: 10.1002/smll.201001229 (2011).

The structural parameters of the sample were investigated by μ-X-ray diffraction (XRD): 35 different spatial points were sampled along the Y-line (**Figure 131a**). With such data, it is possible to obtain the widths (w_b, w_w, **Figure 131c**) and the mismatches (m_b, m_w, **Figure 131d**) of the barrier and of the well by fitting the observed patterns (**Figure 131b**) [2]. Both w_b and w_w undergo a modulated increase moving from field to SAG regions: this is the direct measure of the material enrichment in the SAG region. Moreover, both m_b and m_w values increase almost monotonically moving from the field to the SAG reflecting the expected modulation of the $Al_xGa_yIn_{1-x-y}As$ composition of barrier and well layers.

This key information, coupled with the μm-determination of the energy gap by photoluminescence, led to a characterisation of the structural gradient of the MQW structure along the Y-line from the field to the SAG region.

In summary, we determined the composition and the structure of the SAG EML device with a spatial resolution of 2 μm. This unprecedented characterisation allowed us to understand the structure and thus it gave the appropriate feedback needed to improve the growth process; such development was previously based only on a trial and error approach. A new generation of devices may be produced by extending this method to other SAG growths with different stripes and opening sizes [3,4].

Principal publication and authors
M. Fratini (a,b), N. Poccia (a), A. Ricci (a), G Campi (a,c), M. Burghammer (d), G. Aeppli (e) and A. Bianconi (a), *Nature* **466**, 841-844 (2010).
(a) Physics Department, Sapienza University of Rome (Italy)
(b) Current address: Institute for Photonic and Nanotechnologies, CNR, Roma (Italy)
(c) Institute of Crystallography, CNR, Roma (Italy)
(d) ESRF
(e) London Centre for Nanotechnology and Department of Physics and Astronomy, University College London (UK)

Imaging scale-free structural organisation of oxygen interstitial atoms favouring high temperature superconductivity

A new experiment using a focussed micro X-ray beam has found a surprising pattern lurking in a high temperature superconductor showing that high temperature superconductivity belongs to the class of collective "Quantum Phenomena in Complex Matter". The experiment was performed at beamline **ID13.** We studied a layered oxide of copper belonging to the class of metallic ceramics that held the record for operating at the highest temperature when researchers discovered the superconductivity of this material. Oxide-based superconductors are very difficult to study owing to their extra (interstitial) or missing (vacancy) oxygen atoms, called dopants, which are known to roam around in the skeleton of the material, formed by other elements, and that may freeze in ordered or random patterns when the samples are cooled. The reason for this material's elevated high-temperature conductivity was, until now, not known. For many years scientists assumed that it was because of a homogeneous distribution of dopants, which made researchers concentrate on the nanometre arrangement of these dopants to find the answer to the superconductivity. We have focussed on structure at the nanometre scale as the determinant of the unusually strong superconductivity of the oxides of copper. We used the new technique of X-ray microscopy to examine a copper oxide superconductor whose internal structure could be changed via simple heat treatments – an approach employed by ceramicists over millennia to modify oxide materials. We discovered that the best superconductivity was obtained when the microstructure was most 'connected', meaning that it is possible to trace a path with the same nanostructure (exhibited by oxygen atoms) over a large distance. The microstructure in this case was 'fractal': if we were to zoom in on the material's structure at increasing levels of magnification, its appearance would remain the same (see **Figure 132**).

To see whether the fractal pattern was important, we interfered with it by heating and then quickly cooling the superconductor. Crystals with stronger fractal patterns performed better as a superconductor at higher temperatures than those with weaker fractal patterns. The high temperature conductivity was